Regional Studies in Marine Science 34 (2020) 101065

Contents lists available at ScienceDirect

Regional Studies in Marine Science

journal homepage: www.elsevier.com/locate/rsma

Uncommon biological patterns of a little known endemic Mediterranean skate, *Raja polystigma* (Risso, 1810)

Cristina Porcu *, Andrea Bellodi, Alessandro Cau, Rita Cannas, Martina F. Marongiu, Antonello Mulas, Maria C. Follesa

Dipartimento di Scienze della Vita e dell'Ambiente - Università di Cagliari, 09126 Cagliari, Italy
CoNISMa Consorzio Nazionale Interuniversitario per le Scienze Mare, 00196 Rome, Italy

ARTICLE INFO

Article history:
Received 18 February 2019
Received in revised form 9 January 2020
Accepted 9 January 2020
Available online 11 January 2020

Keywords:
Endemic skate
Age
Growth
Reproduction
Mediterranean Sea
Raja polystigma

ABSTRACT

Rare and poorly studied species, like the endemic skates of the Mediterranean Sea, are considered prone to high rates of extinction and threat because of non-optimal reporting and sampling, which reduce the power of analyses. In this regard, the goal of this study was to establish some basic life-history parameters, unknown to date, of one of these endemics, *Raja polystigma*, caught as by-catch from experimental and commercial hauls in the Mediterranean Sea. Sexes were equally distributed with no major differences in sizes. The age and growth were assessed through *annuli* counts of vertebral *centra* from a sub-sample of 184 individuals. Among different growth models applied to the length at-age-data, the logistic function provided the best fitting curve (L_∞: 691.49; k: 0.26; IP: 4.03 years). The oldest female and male were aged 11 (590 mm LT) and 8 years (521 mm TL), respectively. The estimated longevity was 10.6–15.4 years for females and 7.7–11.2 years for males. Females and males matured at about the same size (L_{50} 506.1 mm TL and 488.1 mm TL, respectively), showing an uncommon pattern among Rajidae. A clear reproductive seasonality was observed during spring and summer. Depth influenced the distribution pattern of *R. polystigma* which appeared to complete its life cycle in coastal waters, with mature adults found exclusively in the shallows and immature specimens in the whole bathymetric range. Given its dependence on the coastal environment and its peculiar life-history features, measures to alleviate anthropic effects on this habitat are urgently needed.

1. Introduction

Despite representing only 0.32% of the oceans' surface, the Mediterranean Sea is a hotspot of marine biodiversity containing on average 6.4% of the world's marine species, of which approximatively 20.2% are endemic (Coll et al., 2010).

Out of 73 chondrichthyans, 15 species of skates (Rajifomes: Rajidae) are currently identified in the Mediterranean Sea, three of which are classified as endemic and found nowhere else: the Maltese skate *Leucoraja melitensis* (Clark, 1926), the Rough skate *Raja radula* Delaroche, 1809, and the Speckled skate *R. polystigma* Regan, 1923 (Dulvy et al., 2016). In this regard, rare and poorly studied species, such as endemic Mediterranean skates, are therefore prone to high rates of extinction and threat (McKinney, 1999) also because of non-optimal reporting and sampling that could affect the power of analyses needed for a correct management (Roberts and Hawkins, 1999; Dulvy et al., 2003). *Raja polystigma* is a small-sized skate reported to inhabit soft bottoms on the continental shelf and upper slope of the western Mediterranean Sea, in the Sicilian Channel and Adriatic Sea (Serena, 2005; Serena et al., 2010). Specimens of the Speckled skate have been frequently misidentified as *R. montagui* Fowler, 1910 due to the high level of external morphological similarity observed both in juveniles and adults (Ramírez-Amaro et al., 2018). Therefore, the resulting lack of accurate species-specific landing data represented a significant issue in knowing the size of the population and in developing proper conservation and management measures. Recent molecular genetic tools were useful to describe their differential geographic distribution. Indeed, *R. polystigma* is present and abundant only in the central-western Mediterranean basin (showing the presence of a single, almost panmictic population) and with *R. montagui* found exclusively in the westernmost area of the Mediterranean (Algerian basin) and in the Atlantic Ocean (Cannas et al., 2008; Frodella et al., 2016; Ramírez-Amaro et al., 2018). The population genetic features of this species, besides their intrinsic vulnerability as *K*-selected strategy species (Ellis et al., 2010), render these organisms highly vulnerable to fishing

* Corresponding author.
E-mail address: cporcu@unica.it (C. Porcu).

https://doi.org/10.1016/j.rsma.2020.101065
2352-4855/

pressure, and thus, calling for focused regional studies to better understand its life-history traits and population status.

Elasmobranchs constitute a common by-catch fraction of many fisheries in the Mediterranean Sea (Ferretti and Myers, 2006). Furthermore, while species targeted by professional fisheries have often been intensely studied, by-catch species such as *R. polystigma* are often ignored. In particular, in Sardinia (Italy, central-western Mediterranean) even if sharks and other chondrichthyans are not the target of fisheries, they are often caught as by-catch and then may be discarded (Marongiu et al., 2017). *Raja polystigma*, in Sardinian bottom trawling fishery, is, among Rajiformes, the second most abundant species found between 10 and 800 m of depth (Density Index, 38.7 $\pm$ 13.0 N/km^2) and the first one in the continental shelf (<200 m, Density Index, 53.2 $\pm$ 25.5 N/km^2) (Marongiu et al., 2017; Follesa et al., 2019a).

Nevertheless, life-history information on *R. polystigma* population is very limited and is needed as input to formulate fishery management decisions. Currently, the only available data are from biological studies carried out along Tunisian coasts more than 30 years ago (Capapé and Quignard, 1978) on the reproductive cycle and in the Balearic Sea on its feeding ecology (Valls et al., 2011; Mulas et al., 2019). Despite the paucity of natural history data, the species is listed as of *Least Concern* according to the International Union for the Conservation of Nature (IUCN) Red List criteria (Dulvy et al., 2016).

In this context, a new knowledge of life-history traits allows the construction of age-based population models and, considering other ecological aspects like reproductive cycle and size at maturity, can eventually lead to an assessment of the population status of this data poor species (Cortés, 2002).

In addition, looking at different reproductive trends among skates like seasonality and bimaturism (e.g., Mabragaña et al., 2015; Porcu et al., 2015), detailed knowledge on these aspects is required to provide sound scientific advice for the implementation of conservation and management strategies.

Given its abundance as by-catch of small and large professional fisheries, the objective of this research was to establish baseline data, which are mostly unknown, on the Speckled skate providing critical information for this species conservation in order to assess properly its possible vulnerability to such fishing pressure. In particular, we focused on: (i) age and growth through the comparison of different growth models; (ii) estimating maturation, mating and egg-case laying periods; (iii) estimating size at maturity for both sexes and describing the morphological changes in reproductive organs during maturation; (iv) testing a possible bathymetric segregation with respect to sex and sexual maturity.

2. Materials and methods

2.1. Sampling

We conducted the study in Sardinian seas (central-western Mediterranean) between 2005 and 2017 at depths between 18 and 660 m through both commercial and scientific (MEDITS) trawl surveys (Fig. 1).

From each *Raja polystigma* individual, the total length (TL, mm), the total weight (TW, g) and the sex were noted.

The population sex-ratio (SR, females:males) was calculated and the significance of its deviation from the 1:1 condition was tested as a null hypothesis through the χ^2 test (Zar, 1999).

2.2. Processing the ageing structures

For ageing purposes, all Speckled skate specimens caught from 2013 were used. A portion of the vertebral column, including 8–10 *centra*, was extracted from the thoracic region of 184 individuals (97 females and 87 males, ranging from 115 to 590 mm TL and

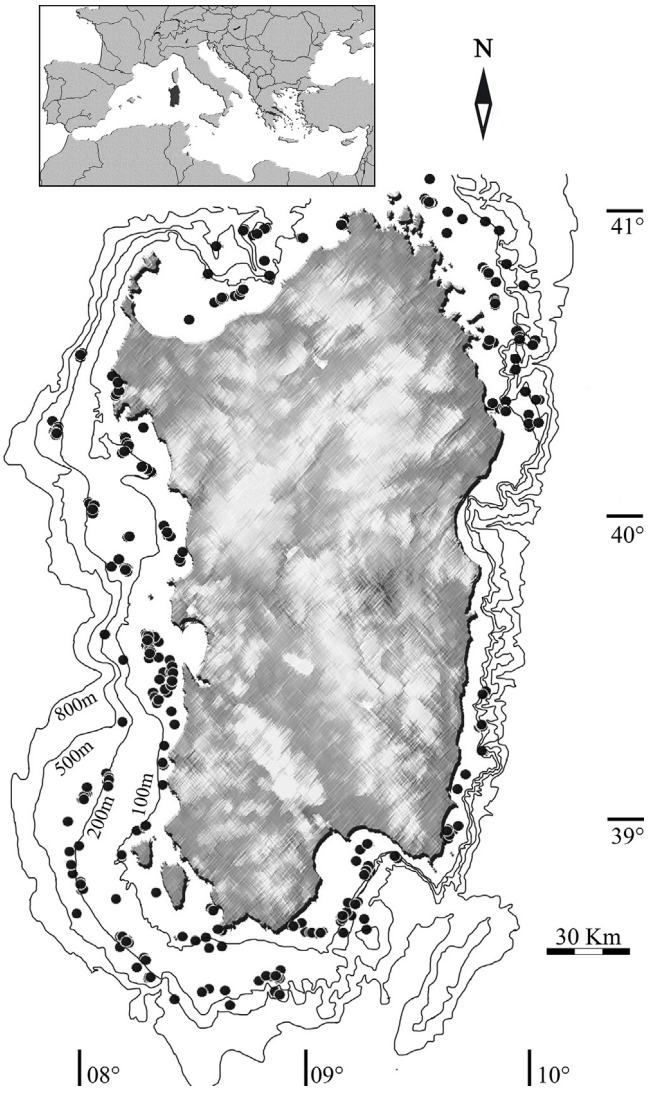

Fig. 1. Map of the study area. Black dots indicate the sampling sites of *R. polystigma* in Sardinian waters (central-western Mediterranean Sea).

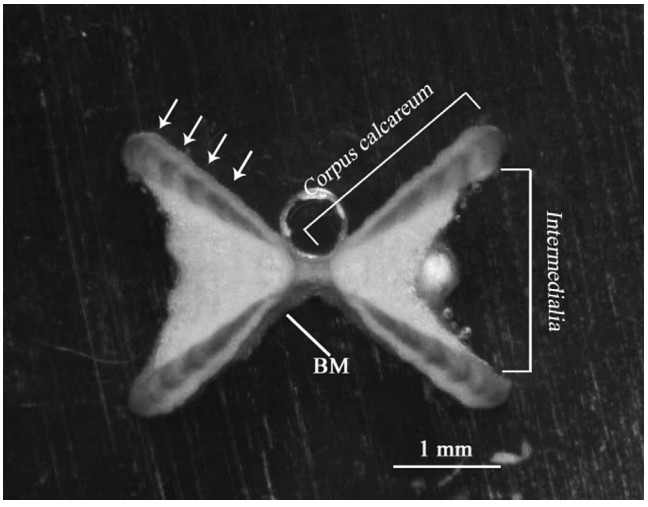

Fig. 2. A vertebral *centra* sagittal section of *R. polystigma* (TL = 356 mm, male) (BM, birth mark). White arrows indicate translucent bands.

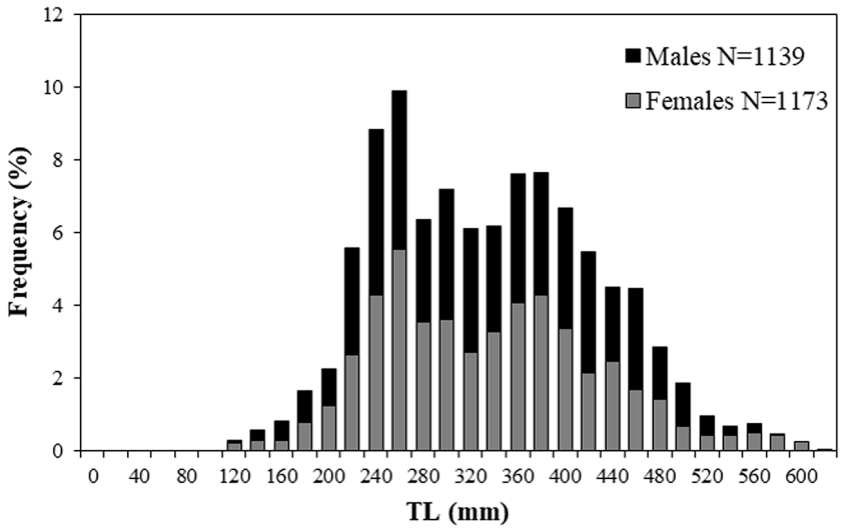

Fig. 3. Total length frequency distributions of male and female *R. polystigma* in the central-western Mediterranean Sea.

118 to 515 mm TL, respectively). In order to remove the excess of soft tissue, firstly the neural and haemal arches were detached using a scalpel, then each *centrum* was soaked in a 5% hypochlorite solution for 5–10 min (Goldman, 2005), depending on the *centra* dimension. *Centra* were then dried and photographed with a Pixelink camera (Pixelink microscope camera PL-A686C annexed to a stereomicroscope (Zeiss Stemi 2000-C)). Through the software tpsDig2 (Rohlf, 2005), the mean vertebral radium (VR, mm) of each individual was recorded. An ANOVA test was then employed to emphasize differences in VR-TL relationship between sexes. Cleaned *centra* were embedded in bi-component epoxy resin (Bio Optica, Technovit EPOX) and mounted on a microscope slide and ground using a polisher (ATM Saphir 320) equipped with progressively thinner abrasive discs (320, 500 and 800 grit). The final product of the grinding process was a vertebral section (sagittal) with a final thickness of about 0.5 mm. This thickness level was chosen because it better allows band visibility under a stereomicroscope. After, a method that could allow the best band visibility was identified. Three different *centra per* sample were selected from a subsample of 12 individuals (6 per sex), and treated with two of the most common staining methods known in literature, Alizarine red (LaMarca, 1966) and Silver Nitrate (Stevens, 1975; Caillet et al., 1983), and tested against the third *centrum* kept unstained. Lastly, each section was photographed with the same equipment cited before and, the images were then converted to grey-scale and processed as suggested by Campana (2014), increasing their contrast and sharpness in order to enhance growth band readability.

2.3. Age estimation, reading precision and growth modelling

Since the growth estimation process through the band count has not been validated yet for the Speckled skate, the band pairs in this paper were assumed to be *annuli*. An *annulus* was defined, following Sulikowski et al. (2003), as the pairing of an opaque and hyaline band. Age was assigned to each vertebral section following the ageing scheme proposed for elasmobranchs by Carbonara and Follesa (2019).

Each section age was estimated by two experienced readers independently and without any knowledge of the skate's gender or size. Both readers replicated the *annuli* counts three times. The band counts started from the first band pair easily recognizable after the Birth Mark (BM), identified as the first clear mark corresponding to an angle change in the *Corpus Calcareum* shape (Sulikowski et al., 2003) (Fig. 2).

The overall reading precision and accuracy were evaluated by the Index of Average Percent Error (IAPE) (Beamish and Fournier, 1981) calculated as $IAPE = N^{-1}\sum\left[R^{-1}\sum\left(|X_{ij}-X_j|\right)X_j^{-1}\right]100$, N equals the number of aged samples, R represents the number of readings, X_{ij} is the ith age determination of the jth fish and X_j equals the average age calculated for the jth fish. In addition the Coefficient of Variation (%CV) (Chang, 1982) and the Percentage of Agreement (PA) were also used. Finally, a Bias test according to Eltink (2000) was performed to evaluate the bias degree between readers.

Only the readings obtained from *centra* treated with the staining method that achieved the best results in terms of accuracy and reproducibility were used for the growth modelling. Growth models were calculated exclusively for age-at-length data obtained from only the *centra* with four out of six consistent readings and a maximum discrepancy of two years (Sulikowski et al., 2003). Using the software Growth II (Henderson and Seaby, 2006), four different growth models were applied to age-at-length data. Among these models, two were chosen because they provide a simple curve describing a linear decrease in somatic growth over time: the von Bertalanffy (3 VBGF) (von Bertalanffy, 1938) and the exponential (2 VBGF) (Fabens, 1965) functions; while the other two employed models were chosen as they offer a sigmoid curve typically defining a two-phases growth: the Gompertz (Winsor, 1932) and the logistic (Richards, 1959) functions. Here each growth function equation is reported: 3 VBGF $TL = L_\infty(1 - e^{-k(t-t_0)})$; 2 VBGF $TL = L_\infty - (L_\infty - \beta)\, e^{[-(kt)]}$; Gompertz $TL_t = L_\infty e^{e^{-k(t-I)}}$; logistic $L_t = L_\infty/1 + e^{-k(t-I)}$ where L_∞ represents the species theoretical maximum length, k is the growth coefficient; t is the observed age, t_0 is the hypothetical age of an individual with TL = 0; β is $(L_\infty - L_0)L_\infty^{-1}$; L_0 is the individual length at birth and finally I is the age at the curve inflection point. Every growth curve was calculated for combined sexes, and for females and males separately. In addition, an ANCOVA test was performed to investigate for possible differences in female and male age-at-length data.

Lastly, in order to evaluate which of these growth models was able to provide the best fitting result to the observed data, the Akaike's Information Criterion (AIC; Akaike, 1974; Haddor, 2001) was calculated for each of them.

2.4. Longevity estimation

Following Barnett et al. (2013), a lower (ω_L) and an upper range (ω_U) of longevity were defined for females and males separately. The lower range was obtained as $\omega_L = T_{max}\,(1 - T_{max}E)$

and the upper range was calculated as $\omega_U = T_{max}(c + E)$ where T_{max} is the maximum observed age, E is the IAPE value calculated using exclusively the empirical data from the greatest 20% of the age classes observed and c is an arbitrary constant ($c = 1.4$) to account for the probability that the absolute maximum age was not observed.

2.5. Reproductive features

In order to describe the maturation process, the reproductive organs and biometric data of both sexes were investigated separately *per* maturity stage. From each specimen, the inner clasper (right) length (CL) in males and the oviducal gland width (OGW) in females were measured (mm). ANOVA was used to test the null hypothesis of no significant difference between maturity stages in the OGW, in females and in the CL, in males.

Maturity for male and female *R. polystigma* was assessed based upon visual inspection of the reproductive organs following the MEDITS handbook (A.V.V.A., 2016; Follesa and Carbonara, 2019; Follesa et al., 2019b) which classifies females into six stages (F1, immature–virgin; F2, maturing; F3A, mature; F3B, mature extruding; F4A, resting; F4B, regenerating) and males into five ones (M1, immature–virgin; M2, maturing; M3A, mature; M3B, mature active; M4, resting).

In particular, maturity status for females was based upon the development of the *uteri*, oviducal glands, ovaries, and oocytes. Instead, for males it was based upon testis development, seminal vesicle, inner clasper length and calcification (Table 1).

The reproductive period was estimated through an analysis of the seasonal distribution of the percentage of maturity stages of females and males.

The ovarian fecundity was defined as the total number of yolk-filled follicles in both ovaries (Porcu et al., 2015) released *per* mature female during the spawning period. The diameters (mm) of yolk follicles were also recorded.

First maturity was considered to be the size (TL) of the smallest mature *R. polystigma* examined for each sex. L_{50} (size at maturity = length at which 50% of the individuals are mature) and the maturity range ($MR = L_{75}–L_{25}$) were estimated by fitting maturity ogives to the proportion of mature individuals in each 20 mm TL size class for both sexes separately and using a binomial generalized linear model (GLM, R Core Team, 2017) with a logistic link (ICES, 2008). Non-linear least square regression was used to estimate the parameters: $p = 100\{1 + \exp[a + bTL]\}^{-1}$, where p is the proportion of mature fish at TL size class, a is the intercept and b is the slope of the maturity curve. The length at maturity is $L_{50} = (-a/b)$. In addition, logistic regression was used to determine the length at maturity ogive of extruding females (carrying egg-cases) (L_{50EXT}).

In a similar way, a logistic model was fitted to the paired maturity and age data, and the age at which 50% of individuals are sexually mature (A_{50} and A_{50EXT}) was calculated following the equation: $p = 100\{1 + \exp[a + bAge]\}^{-1}$.

2.6. Segregation patterns

Sex (female:male) and maturity of both sexes (immature female:mature female; immature male:mature male) ratios were examined at five depth strata where the species's presence was recorded (D1 = 18–51 m; D2 = 51–100 m; D3 = 101–200 m; D4 = 201–500 m; D5 = 501–660 m; strata A, B, C, D and E of the MEDITS programme respectively) with Pearson tests (χ^2) to detect deviations from the 1:1 ratio.

A non-metric Multidimensional scaling analysis (nMDS) was performed using the Bray–Curtis similarity index (Primer v.6 software, Clarke and Gorley, 2006) in order to examine segregation patterns on the basis of maturity stages and depth strata. The observed differences were tested using an analysis of the similarity randomization test (ANOSIM).

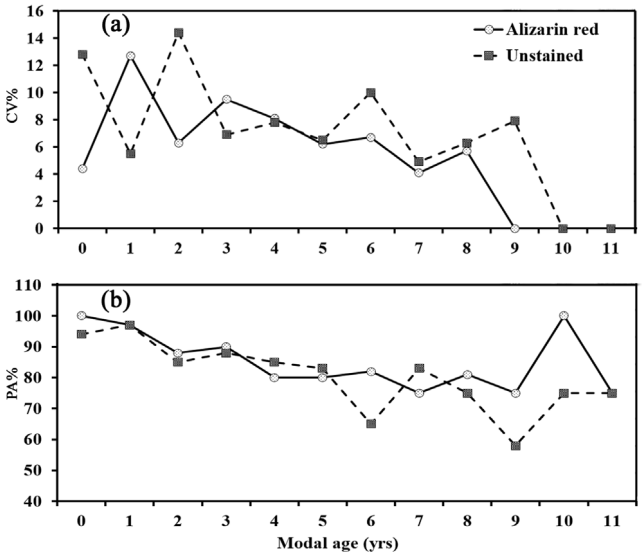

Fig. 4. The %CV (a), PA (b) of readings carried out on unstained and Alizarin red stained vertebral *centra* plotted against the modal age.

3. Results

3.1. Sex ratio and length frequency distributions

Of the 2312 specimens of *Raja polystigma* collected, 1173 were females and 1139 were males; sexes were equally distributed: SR = 1.03; $\chi^2 = 0.25$; $p > 0.05$.

In females, the TL ranged from 103 to 600 mm (mean ± S.D. = 326.28 ± 93.29) and TW from 5.58 to 1580.0 g (mean ± S.D. = 225.60 ± 231.46) and in males, the TL ranged from 112 to 610 mm (mean ± S.D. = 327.31 ± 90.97) and TW from 6.86 to 1480.0 g (mean ± S.D. = 214.41 ± 198.91) with both females and males attaining substantially the same size (Fig. 3). The results from Kolmogorov–Smirnov two-sample test did not indicate a statistically significant difference in length-frequency distribution between sexes (K–S test = 2.19; $p > 0.05$).

3.2. Age estimation, reading precision and growth modelling

The vertebral radius (VR) and the individual TL appeared to be linked by a linear relationship in both sexes. The obtained regression lines for females ($b = 0.2175$; $a = 0.0043$; $r^2 = 0.8749$) and males ($b = 0.1414$; $a = 0.0004$; $r^2 = 0.9212$) have proved to be significantly different (ANOVA, F-ratio = 534.14; $p < 0.000$; $r^2 = 0.90$).

Among the investigated staining methods, the silver nitrate did not seem to provide an acceptable increase in band visibility. While, Alizarin red and the observation of unstained *centra* offered an equally good level of growth band clarity from the preliminary observation of the subsample *centra*. For this reason, an entire reading cycle (with 3 repetitions) was conducted at first on all the *centra* kept unstained and then on the same *centra* stained with Alizarin red.

The band counts carried out on the unstained *centra* achieved a high level of reading precision and reproducibility (IAPE = 5.96%; PA = 86.6%; %CV = 7.9). In Fig. 4a, the PA and %CV values for the single modal ages were shown. No signs of bias were detected by the bias test ($z = -0.257$). Of the total vertebral *centra* analysed only 16 (8.7%) were discarded due to their reading variability (not being identified with the same age at least 4 times out of 6).

The age estimation process carried out on Alizarin red stained samples provided even slightly better results in terms of reading

Table 1
Macroscopic maturity scales of oviparous Elasmobranchs. F, Females; M, Males.

Sex	Reproductive apparatus aspect	Maturation state	Stage
F	The ovary with small isodiametric eggs is barely discernible. The distal part of oviducts is thick-walled and whitish. The oviducal glands are less evident.	Immature virgin	1
M	Claspers are small and flaccid, and do not reach the posterior edge of the pelvic fins. The sperm ducts are not discernible. The testis is small and narrow.		
F	The whitish and/or a few yellow maturing eggs are visible in the ovary. The distal part of the oviducts (uterus) is well developed but empty. The oviducal glands are small.	Maturing	2
M	The claspers are larger, but the skeleton is still flexible. They extend to the posterior edge of the pelvic fins. Sperm ducts are well developed and eventually begin to meander.		
F	The ovaries contain yellow eggs (large yolk eggs). The oviducal glands are enlarged, and oviducts are distended.	Mature	3A
M	The claspers extend well beyond the posterior edge of the pelvic fin, and their internal structure is generally hard and ossified. The testes are greatly enlarged. The sperm ducts meander over almost their entire length.		
F	The ovary walls are transparent. Oocytes are of different sizes, white or yellow. The oviducal glands are large. The egg-cases are more or less formed in the oviducts (extruding stage).	Mature extruding/active	3B
M	The claspers are longer than the tips of the posterior pelvic fin lobes; the skeleton has hardened and pointed axial cartilages. The sperm ducts are large. Sperm flows on pressure from the cloaca (active stage).		
F	The ovary walls are transparent. The oocytes are of different sizes, white or yellow. The oviducts appear much enlarged, collapsed and empty. The diameter of the oviducal glands is reducing.	Resting	4A
M	The clasper is longer than the tips of the posterior pelvic fin lobes; the skeleton has still hardened axial cartilages. The sperm ducts are empty and flaccid.		
F	The ovaries are full of small follicles similar to stage 2, enlarged oviducal glands and uterus.	Regenerating	4B

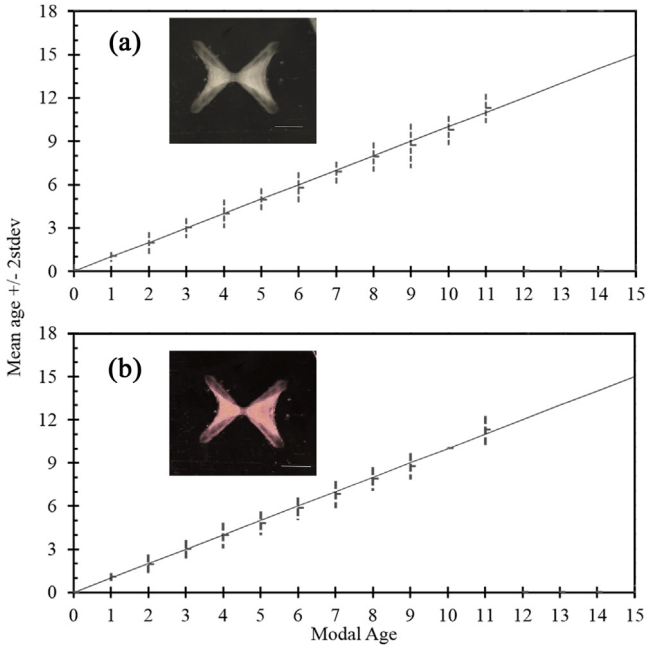

Fig. 5. Age bias plot, recorded for readings carried out on unstained (a) and Alizarin red stained *centra* (b), with the mean age ± 2 S.D. recorded for all readers combined, plotted against the modal age. The estimated mean age corresponds to modal age if the estimated mean age is on the 1:1 equilibrium line (solid line). Relative bias is represented by the age difference between estimated mean age and modal age. Scale bar, 1 mm. (For interpretation of the references to colour in this figure legend, the reader is referred to the web version of this article.)

precision and reproducibility (IAPE = 5.17%; PA = 86.8%; %CV = 7.0). Also in this case, the test revealed no signs of bias (z = −0.765). Only 8 (4.35%) *centra* out of the 184 analysed were discarded due to their reading variability, the remaining 176 comprised 92 females (ranging from 115–590 mm in TL and 0–11 years) and 84 males (ranging from 118–515 mm in TL and 0–8 years).

The analysis of CV and PA values for each age class (Fig. 4a,b) showed a slightly lower error level and, consequently, a higher agreement degree for the readings carried out on Alizarin red stained *centra*. This situation seemed particularly true for the oldest age classes (>4 years).

Furthermore, the age-bias plot revealed a similar situation, with the readings obtained from the Alizarin red stained *centra* (Fig. 5b) exhibiting a lesser variability level than those obtained from unstained samples (Fig. 5a). The discrepancy between the two methods appeared greater as regards the oldest age classes.

Given these results, the growth functions were fitted on age-at-length data obtained exclusively from Alizarin red stained vertebral *centra*.

Among the tested growth models in the present study, the logistic function provided the best fit to the observed data, as reported by the AIC both for combined sexes and for females and males separately (Table 2, Fig. 6a,b). The AIC revealed also that S-shaped functions seemed to be more appropriate to describe the Speckled skate growth. The Gompertz function presented the second best result in terms of fitting to the age-length data (Table 2). On the other hand, given their higher AIC values, the two simple-shaped functions, the common von Bertalanffy (3 VBGF) and the 2 VBGF, appeared less accurate for the species growth description.

Moreover, the S-shaped functions stated a higher growth rate and, therefore, lower L_∞ than those reported by the 3 VBGF and the 2 VBGF ones.

However, each investigated model showed a higher k value in males than in females suggesting a faster growth rate in males.

3.3. Longevity estimation

The IAPE value calculated for the greatest 20% of the age classes was 2.97% for females and 4.31% for males. For this reason, the upper (ω_U) and the lower (ω_L) range were estimated to be 15.4 and 10.6 years, respectively, for females and males. The estimated longevity for males ranged, instead, between 11.2 (ω_U) and 7.7 (ω_L) years.

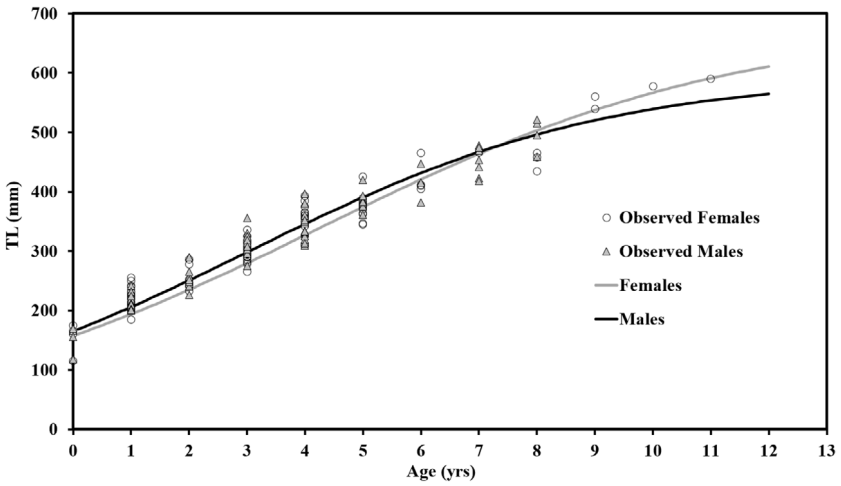

Fig. 6. Logistic growth curves calculated for *R. polystigma* females and males separately.

Table 2
R. polystigma growth parameters (mean ± S.E.) calculated from four models for combined sexes and for females and males separately. Values from the best fitting model are reported in bold.

Growth model	L_∞ (mm)	k	t_0 (years)	Min. size (mm)	IP (years)	AIC
Combined sexes						
3 VBGF	784.82 ± 12.2	0.11 ± 0.004	−1.718 ± 0.25	–	–	1095.33
2 VBGF	784.82 ± 12.2	0.11 ± 0.004	–	136	–	1095.33
Gompertz	715.84 ± 11.6	0.18 ± 0.04	–	–	2.06 ± 0.068	1055.02
Logistic	**691.49 ± 15.2**	**0.26 ± 0.02**	–	–	**4.03 ± 0.147**	**936.329**
Females						
3 VBGF	782.74 ± 78.5	0.109 ± 0.02	−1.96 ± 0.30	–	–	254.367
2 VBGF	782.74 ± 78.5	0.109 ± 0.02	–	151	–	254.367
Gompertz	765.16 ± 25.5	0.16 ± 0.04	–	–	2.82 ± 0.15	136.608
Logistic	**681.18 ± 34.0**	**0.28 ± 0.04**	–	–	**4.29 ± 0.45**	**118.88**
Males						
3 VBGF	645.01 ± 66.2	0.149 ± 0.03	−1.79 ± 0.27	–	–	268.031
2 VBGF	644.84 ± 66.2	0.149 ± 0.03	–	152	–	268.031
Gompertz	622.90 ± 21.7	0.22 ± 0.015	–	–	1.30 ± 0.19	264.825
Logistic	**596.55 ± 24.8**	**0.32 ± 0.019**	–	–	**3.00 ± 0.31**	**264.775**

3.4. Size and age at maturity

According to the maturity criteria herein defined, the smallest mature female and male Speckled skate had a TL of 440 and 396 mm, respectively. Macroscopic L_{50} and the maturity range were 506.1 mm TL (S.E. = 3.60) and 21.15 mm TL (S.E. = 4.12) for females and 488.5 mm TL (S.E. = 3.53) and 44.43 (S.E. = 4.44) for males (Fig. 7a,b). The extruding females, instead, showed a minimum length of 512 mm TL, a L_{50EXT} of 582.7 mm TL (±9.52) and a MR of 52.63 (S.E. = 10.19) (Fig. 7a). Maturity took place at 84%, 97% and 80% of the maximum observed length for mature females, extruding females and mature males, respectively.

Males and females attained an A_{50} of 8.07 (S.E. = 0.12) and 7.34 y (S.E. = 0.12) respectively, while extruding females showed an A_{50EXT} of 10.91 (S.E. = 0.30) (Fig. 7c,d).

3.5. Maturity

Approximately 82% of the male *R. polystigma* were macroscopically classified as immature (112–481 mm TL, 298.0 ± 73.0), 9.5% as maturing (325–545 mm TL, 433.0 ± 36.7 mm), 5% as mature (396–575 mm TL, 473.0 ± 37.4 mm), 2.2% as active (409–570 mm TL, 489.3 ± 36.5 mm) and 1.7% as resting (402–535 mm TL, 471.7 ± 27.9 mm). In females, 76.1% were classified as immature (104–472 mm TL, 291.5 ± 73.1 mm), 20% as maturing (305–493 mm TL, 398.6 ± 46.4 mm), 2.3% and 1.1% as mature (440–570 mm TL, 520.8 ± 35.3) and extruding (512–595 mm TL, 556.5 ± 29.4 mm) respectively and only 1.7% as spent (stage 4A and 4B, 492–592 mm TL, 534.1 ± 31.6 mm) (Fig. 8).

An abrupt increase in the ovary mass (Fig. 9a) corresponded well with the onset of female maturity evaluated macroscopically. Oviducal gland growth appeared slow in immature females, but subsequently fast growing at the mature stages (Fig. 9c) showing statistically significant differences among all stages except for stage 3A and 3B (ANOVA, $p < 0.05$). Similarly, an abrupt change in the testis mass was observed at approximately 440 cm CL (Fig. 9b), corresponding well with a rapid increase in standardized inner clasper length. An initial slow growth in size followed by an acceleration at the beginning of maturation was observed (ANOVA, $p < 0.05$) (Fig. 9d).

The relative frequency of each maturity stage by season, both for females and males, is shown in Fig. 10. During the sampling period, all maturity stages were recorded with some variations in their occurrence. In particular, a predominance of immature female and male specimens was observed throughout the year. Mature and extruding females were found in spring (from late May). Adult spent-resting females were observed during all seasons except for the winter (Fig. 10a). Mature males were present throughout the year with a higher percentage of active specimens from May to June (Fig. 10b).

The ovarian fecundity in mature females varied from 14 to 19 yolked follicles in both ovaries (mean ± S.D., 16 ± 2.3 follicles). There was no significant difference in the number of follicles between the right and the left ovary (paired t-test, $p > 0.05$). The

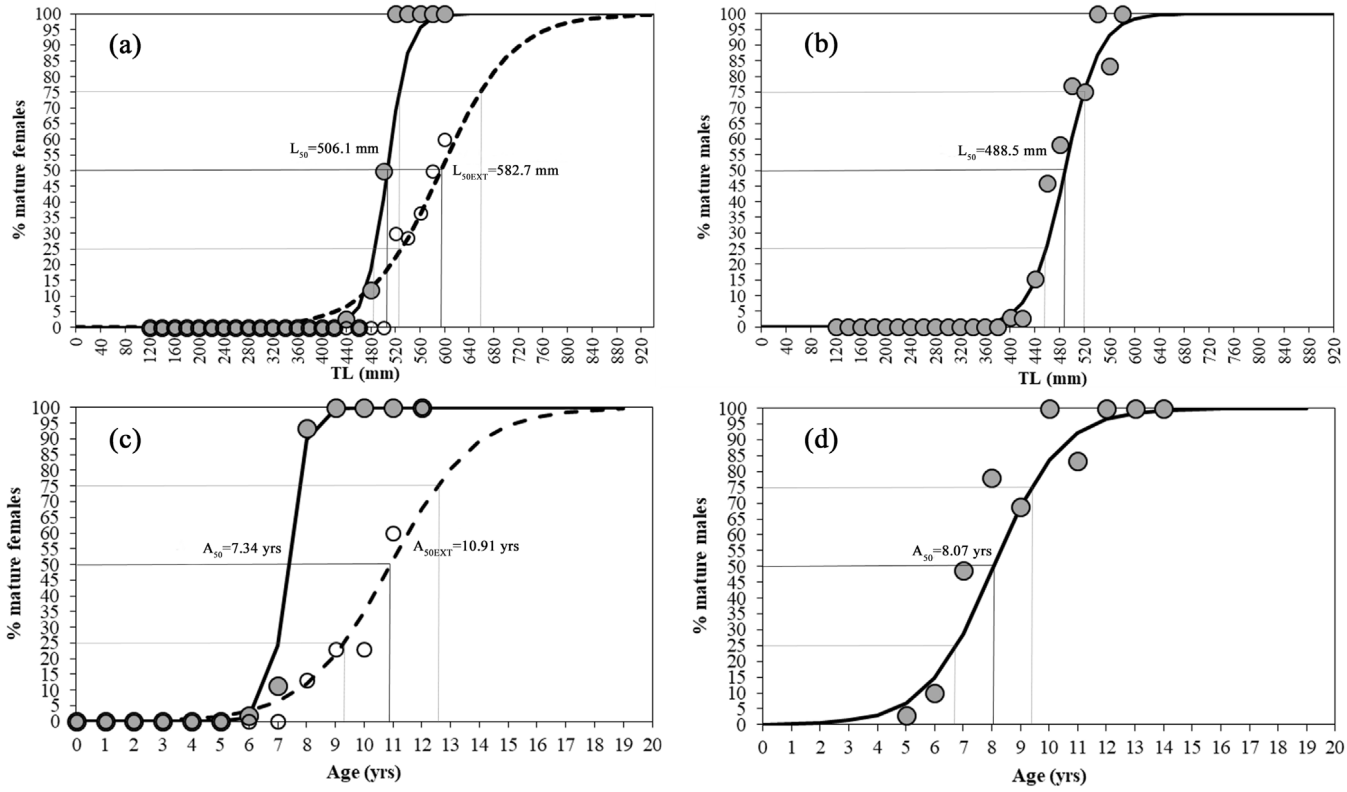

Fig. 7. Proportion of mature toward immature female and male *R. polystigma* in each class of total length (a, c) and age (b, d) in the central-western Mediterranean Sea. Length at 25%, 50%, and 75% maturity determined from fitted logistic curves are indicated by dashed lines.

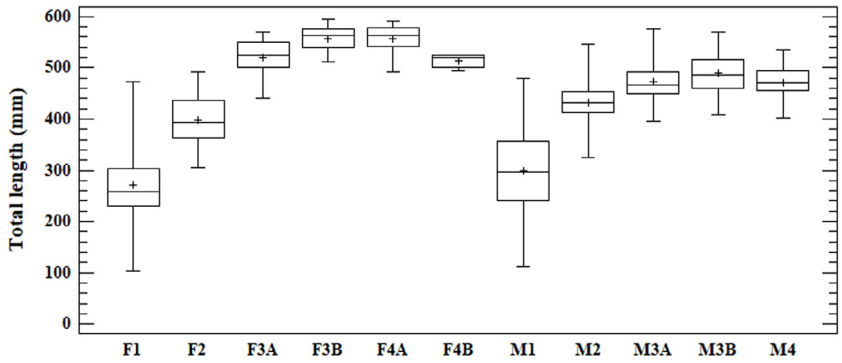

Fig. 8. Box and whiskers plot with the mean, standard deviation, range of total length of both male (M1, immaturev–irgin; M2, maturing; M3A, mature; M3B, mature active; M4, resting) and female (F1, immature–virgin; F2, maturing; F3A, mature; F3B, mature extruding; F4A, resting; F4B, regenerating) *R. polystigma* at each maturity stage.

diameter of vitellogenic follicles varied from 6.8 to 26.5 mm with a mean ± S.D. of 14.38 ± 5.4 mm.

3.6. Segregation patterns

No evidence of segregation by sex was observed. Males and females were equally distributed along the investigated depth range. Furthermore, analysing the maturity, immature females and males dominated in all depth strata (Table 3).

Analysing in detail the maturity condition, immature and maturing females (F1 and F2) and immature males have been found at all levels of depth (D1–D5). However, they seemed to be more common in intermediate waters (D2 and D3, 51–200 m), while maturing males (M2) were distributed in shallower waters (D1 and D2, 18–100 m) (Fig. 11). Mature individuals were observed from 18 to 250 m of depth. In particular, mature females (F3A) and males (M3A) were associated with D1 and D2 strata. Extruding females (F3B) and active males (M3B) were skewed towards shallower waters (D1, <50 m) (Fig. 11a,b).

The multivariate analysis (nMDS) confirmed a clear segregation of the maturity stage highlighting an association of immature specimens (F1 and M1), active male and mature females (M3B and F3A). Specimens in post-spawning seemed to segregate together (Fig. 12) (ANOSIM, $R = 0.82$; $p < 0.01$).

4. Discussion

The present study represents the first assessment of age, growth, maturation and reproduction of the Speckled skate *Raja polystigma*, endemic to the Mediterranean Sea, and therefore contributes towards the limited information available on the species throughout its distribution range.

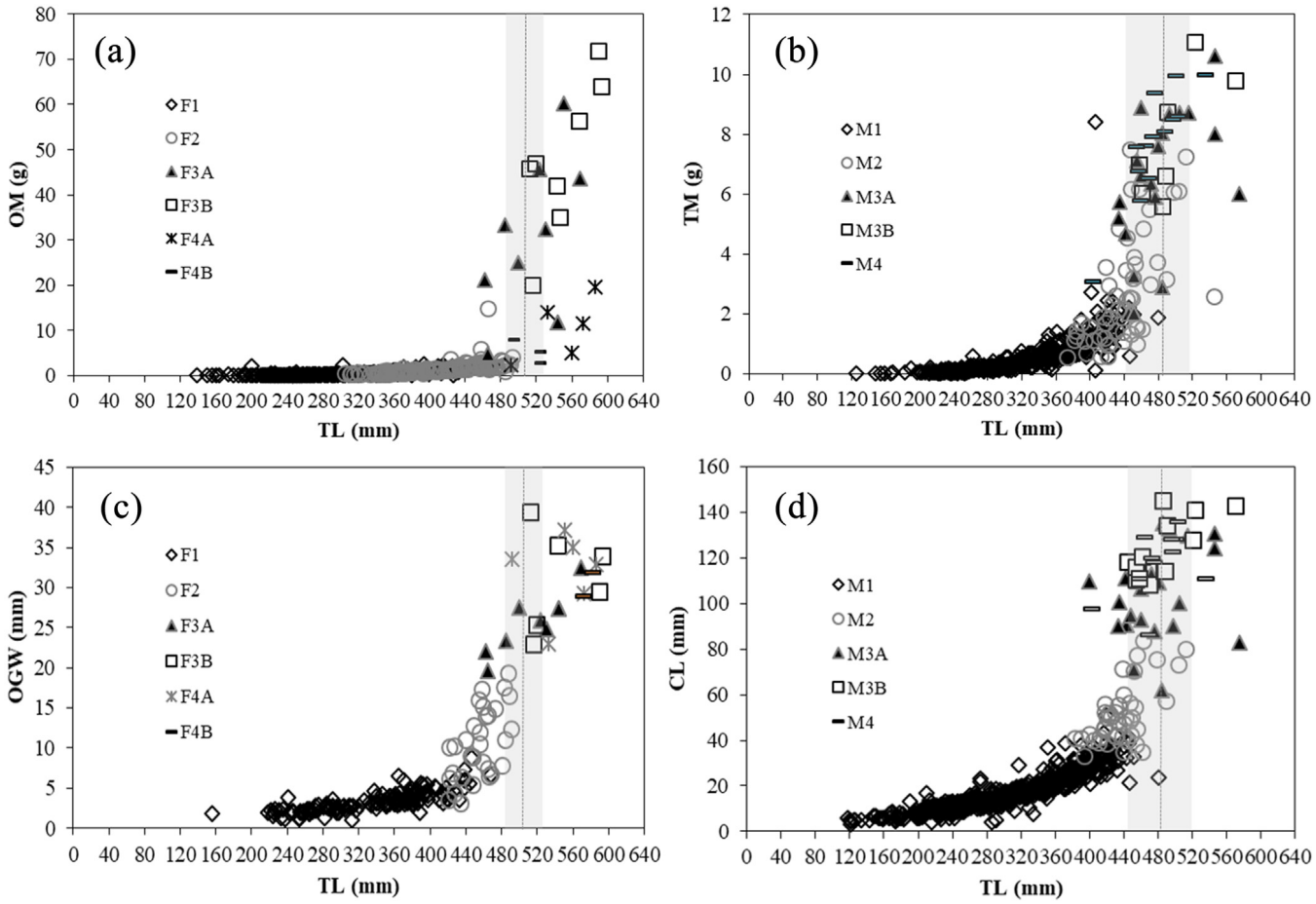

Fig. 9. Relationship between total length (TL) and ovary mass (OM) (a), and oviducal gland width (OGW) (b) in females, and between total length (TL) and testis mass (TM) (c) and clasper length (CL) (d) in males of *R. polystigma*. Dashed line indicates macroscopic L_{50} estimate with 25%–75% mature as grey bar.

Table 3
Total sample size and proportion of females and males, immature (M_I, F_I) and mature specimens (M_M, F_M) in the five depth levels for *R. polystigma* in Sardinian seas (central-western Mediterranean Sea). The p-values (p) are shown for each Pearson chi square test (χ^2) and significant results are in bold ($\alpha = 0.05$).

Depth	N	F:M	χ^2	p	F_I:F_M	χ^2	p	M_I:M_M	χ^2	p
D1	200	0.75	1.7	0.19	2.19	5.42	**0.02**	1.92	5.2	**0.02**
D2	580	0.98	0.01	0.90	12.70	125.79	**0.00**	6.92	93.4	**0.00**
D3	990	1.05	0.2	0.65	100.2	31.38	**0.00**	29.25	267.52	**0.00**
D4	359	1.10	0.31	0.56	–	122.68	**0.00**	170	107.89	**0.00**
D5	30	1.31	0.07	0.80	–	6.17	**0.01**	–	6.21	**0.01**

4.1. Age, growth and longevity

The age estimation process carried out on vertebral *centra* was facilitated by a good level of band visibility. *Annuli* were, in most cases, easily detectable and recognizable. The age estimation process conducted on unstained samples processed with image analysis software (i.e., colour enhancement), as suggested by Campana (2014), obtained a high level of reading precision and reproducibility. However, the same process carried out on the same *centra* stained with Alizarin red, achieved slightly lower IAPE and CV%, and higher PA values, appearing to be an even more suitable technique in order to enhance better growth rings on *R. polystigma* vertebral *centra*. This is particularly true for age estimation in older individuals (>6–7 years), where last bands are often compressed and more challenging to distinguish. For this reason, this protocol is recommended for further studies on Speckled skates before trying other more expensive and time-consuming techniques.

Even though it was not possible to analyse hard structure extracted from unhatched embryos, the observation of *centra* belonging to the smallest free-living Speckled skates of both sexes (115 mm TL and 118 mm TL for females and males, respectively) did not show any sign of growth rings. This particular result suggests that the first band in this species is formed after hatching, as already reported in literature for not oviparous batoids (Mejía-Falla et al., 2014), thus supporting the age estimation process carried out in this work.

As the present study is the first to provide age and growth estimates for *R. polystigma*, no comparisons with other populations is currently possible.

Among chondrichthyans, various growth models have been applied to length-at-age data (Cailliet and Goldman, 2004). The three parameter von Bertalanffy (3 VBGF) is the most widely used for fish including sharks and rays (Cailliet and Goldman, 2004). However, the 3 VBGF does not work properly in estimating growth parameters when sample size is low, especially when lacking small or very large individuals (Cailliet and Goldman,

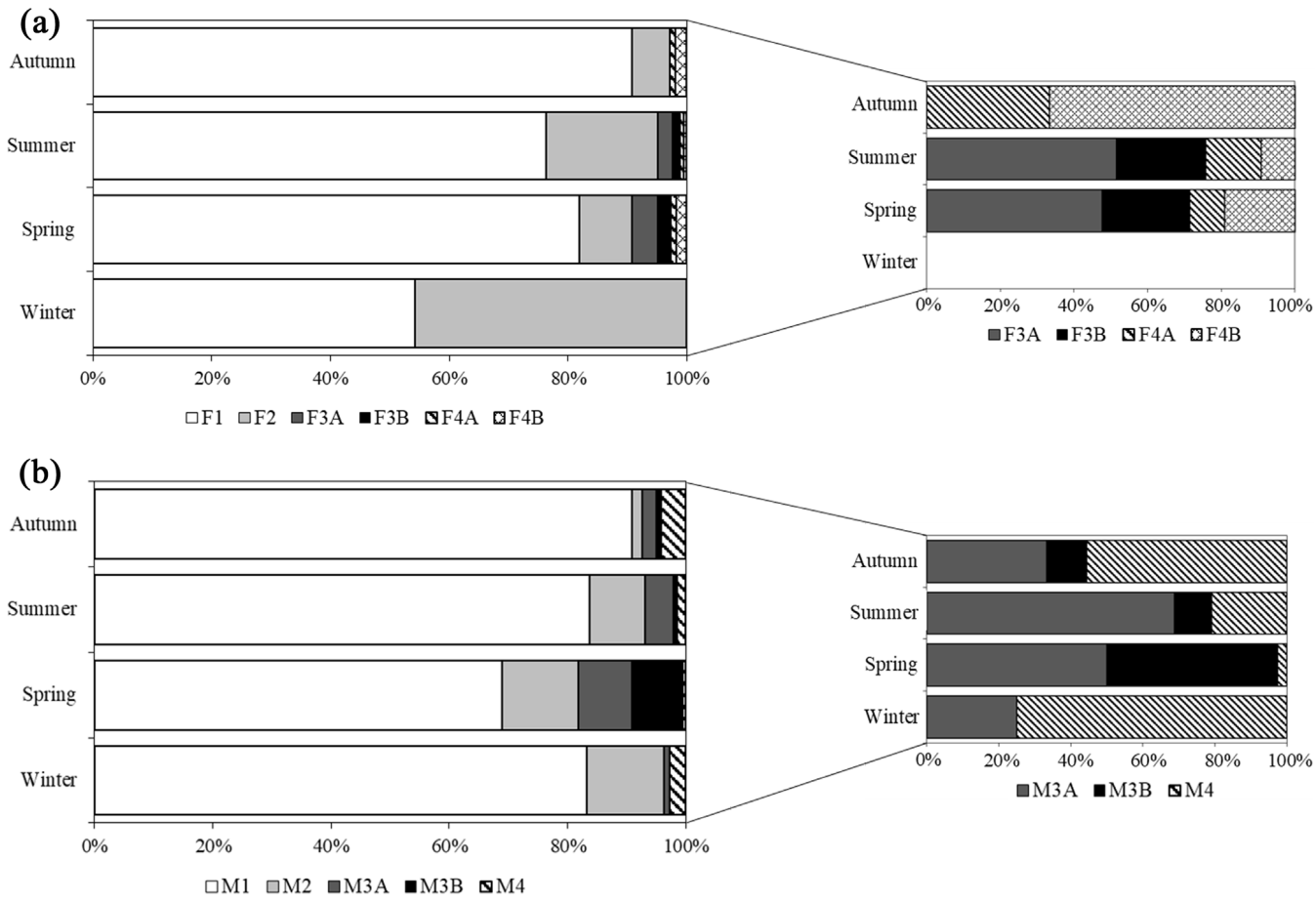

Fig. 10. Seasonal distribution of *R. polystigma* (a) females (F1, immature–virgin; F2, maturing; F3A, mature; F3B, mature extruding; F4A, resting; F4B, regenerating) and (b) males (M1, immature–virgin; M2, maturing; M3A, mature; M3B, mature active; M4, resting) at each maturity stage in Sardinian seas.

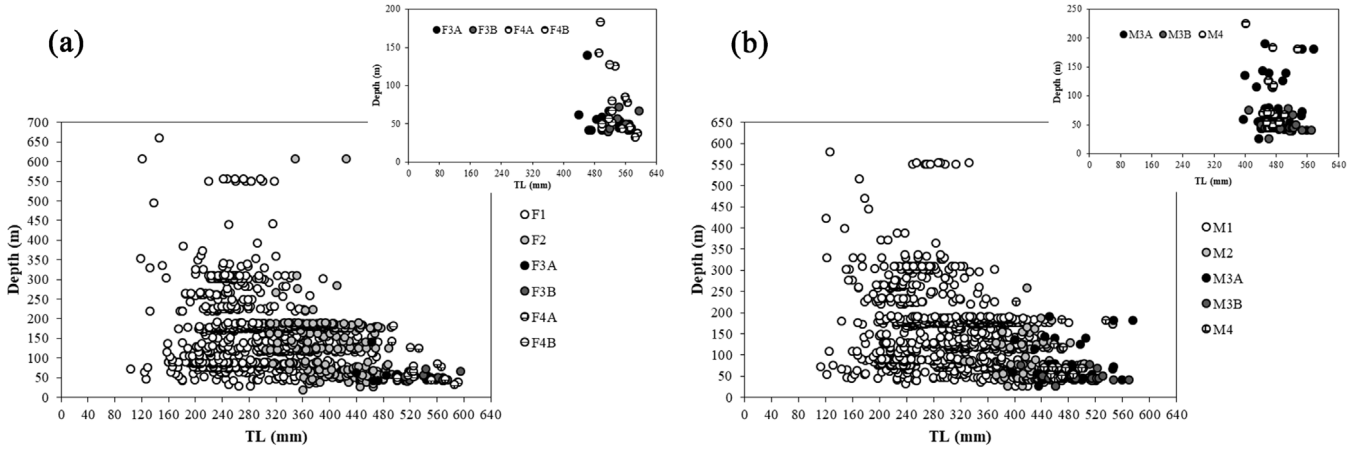

Fig. 11. Length distribution of *R. polystigma* (a) females (F1, immature–virgin; F2, maturing; F3A, mature; F3B, mature extruding; F4A, resting; F4B, regenerating) and (b) males (M1, immature–virgin; M2, maturing; M3A, mature; M3B, mature active; M4, resting) by depth and maturity stage.

2004). An alternative equation to the 3 VBGF replaces the biologically unrealistic variable t_0 (theoretical time when TL is zero) with an estimate of size at birth, L_0, which is often well defined for elasmobranch populations. This alternative equation, the two parameter von Bertalanffy growth function (2 VBGF) provides more realistic growth parameter estimates with small sample sizes (Goosen and Smale, 1997; Thorson and Simpfendorfer, 2009). Additional models that provide sigmoid growth curves (i.e., Gompertz and logistic; Ricker, 1979) are also used to describe elasmobranch age and growth especially if the volume of the organism reflects the growth better than the length (Cailliet and Goldman, 2004).

Although the von Bertalanffy growth curve represents the most extensively used to describe growth in fish, the use of more than one growth function in order to adequately describe the growth of a given species is recommended (Mejía-Falla et al., 2014).

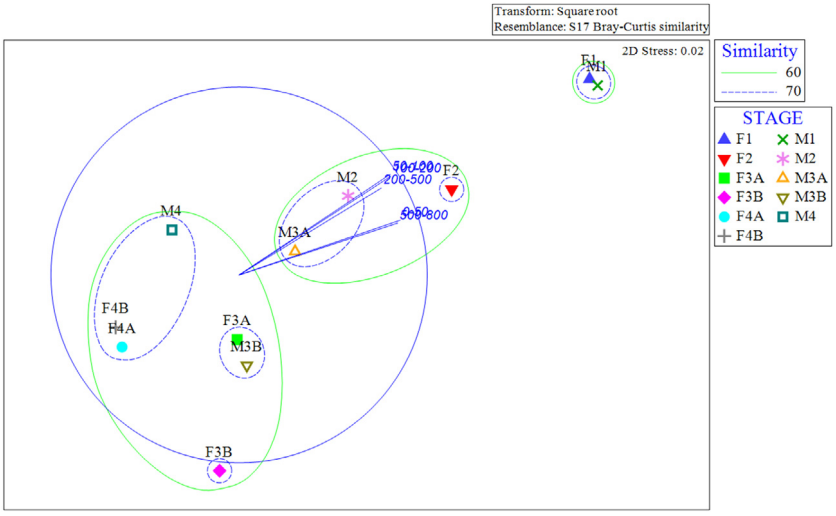

Fig. 12. Non-metric multidimensional scaling plot of *R. polystigma* females (F1, immature–virgin; F2, maturing; F3A, mature; F3B, mature extruding; F4A, resting; F4B, regenerating) and males (M1, immature–virgin; M2, maturing; M3A, mature; M3B, mature active; M4, resting) by depth levels and maturity stage.

Among the four growth models applied to the length at-age-data for *R. polystigma*, those providing an S-shaped growth curve achieved the best result in terms of fitting to the observed data with respect to the VBG type models (3VBGF and 2VBGF). In particular, the logistic function appeared to be the most appropriate model to describe the growth of this Mediterranean endemic species, according to the AIC value. Our results suggest a two-speed growth rate, with a relatively fast growing phase during the first few years, followed by a phase in which growth in length slows while the growth in weight continues (Fisher et al., 2013). This peculiar feature has been already described in literature for other batoids (e.g., *Raja rhina* and *R. binoculata* along the US Pacific coasts, Zeiner and Wolf, 1993; *Beringraja binoculata* in the Gulf of Mexico, Neer and Thompson, 2005; *Rhinoptera bonasus* in US Atlantic waters, Fisher et al., 2013; *Dipturus oxyrinchus* in the Mediterranean Sea, Bellodi et al., 2017).

For the majority of the investigated skate species, a strong sexual dimorphism in size is commonly reported (females attaining bigger sizes than males, e.g., Sulikowski et al., 2007; Yigin and Ismen, 2010; Mulas et al., 2015; Porcu et al., 2015; Bellodi et al., 2017). However, *R. polystigma* showed no major difference in size between sexes, consequently no major differences in asymptotic length (L_∞) were expected, nor found. This particular feature could be related to the overall small size of the species, considering the similar outcome also reported for the small-sized skate *R. miraletus* by Kadri et al. (2012) in the Mediterranean Sea.

With respect to the growth rate, every investigated growth model showed male specimens with higher k values than females. Despite observed differences, the obtained values fall in the growth coefficient range described for batoids (based on VBG model) from 0.1 to 0.3 (Holden, 1974).

Despite the similarities in maximum size among sexes, their discrepancies in growth rates resulted in different Inflection Points (recognized as the point on a curve at which the sign of the curvature changes) in S-shaped growth function for females and males. Indeed, males seemed to reach the IP earlier during their life cycle than females (at 3 years and 4.29 years, respectively). The change in growth trajectories is often associated with the onset of maturity (Araya and Cubillos, 2006). However, the late A_{50} estimated for this species (8.07 years for males and 7.34 for females) suggests that the onset of maturity does not have a role in the growth of *R. polystigma.* It is possible that other events such as changes in habitat or feeding behaviour may cause changes in growth trajectories (Ricker, 1979). For this reason, further studies on those particular aspects of the Speckled skate biology appear to be crucial.

In addition, several papers in the recent literature reported that the classically employed method for the longevity estimation using the k value obtained from the growth curve could easily lead to an overestimation (e.g., Ebert et al., 2009; Barnett et al., 2013; Mejía-Falla et al., 2014). For this reason, the longevity of *R. polystigma* was investigated through the method proposed by Barnett et al. (2013) that provides an upper and lower range of longevity considering the maximum observed size of the species and the reading precision (IAPE) of the older age class. The estimated longevity range for *R. polystigma* in Sardinian seas (10.6–15.4 years for females and 7.7–11.2 years for males) resulted to be slightly lower than that observed in the other small-sized Mediterranean skate as *R. miraletus* (Kadri et al., 2012). This discrepancy could be due to a different methodology employed by these authors.

4.2. Size and age at maturity

Male and female *R. polystigma* matured between 80% and 84%, respectively, of their maximum total sizes, which is consistent with the range reported for other elasmobranchs (60%–90%) (Ebert et al., 2008; McPhie and Campana, 2009). However, the high L_{50} of the extruding females, at 97% of maximum total size, represents a clear indication of vulnerability of this exploited species.

A slight sexual dimorphism in size at maturity has been observed. Indeed, both sexes of *R. polystigma* matured at almost the same size (L_{50} females, 506.1 mm TL and L_{50} males, 488.1 mm TL), showing an uncommon pattern among members of the Rajidae family in the Mediterranean Sea, which display the typical bimaturism with females maturing at larger sizes than males (*D. nidarosiensis*, Follesa et al., 2012; *D. oxyrinchus*, Bellodi et al., 2017; *R. asterias*, Barone et al., 2007; *R. brachyura*, Porcu et al., 2015; *R. clavata*, Kadri et al., 2014; *R. miraletus*, Kadri et al., 2012). This pattern could be due to a lack of selective pressure on females to reach a larger body size, which would increase fecundity (Mabragaña et al., 2015).

4.3. Maturity

The growth profile of all reproductive organs supported the hypothesis that their development follows several distinct phases

as identified in major maturation stages described for other rajids (Ebert et al., 2008; Oddone and Vooren, 2005; Frisk and Miller, 2009) and elasmobranchs in general (e.g., Porcu et al., 2014). Both clasper lengths in males and oviducal gland widths in females increased with increasing total length, similarly to the previous study for this species (Capapé and Quignard, 1978). The abrupt increase in the gonad weight immediately after the onset of sexual maturity, reported in this study, has been observed for other Rajidae species such as *R. brachyura* (Porcu et al., 2015) and *R. miraletus* (Kadri et al., 2012). Furthermore, *R. polystigma* followed the general pattern observed in several rajid species for the relationship between clasper and TL (three-phased sigmoid curve) with the middle phase of the sigmoid representing maturing individuals (e.g., Oddone and Vooren, 2005; Bellodi et al., 2017).

Within Sardinian waters, during the sampling period, all maturity stages were recorded. Mature and egg-case extruding females were found from late May to August, indicating a clear seasonal reproductive cycle, differently from those observed on Tunisian coasts by Capapé and Quignard (1978), where extruding females were found throughout the year and mainly in winter. Reproductively active males, however, occurred in all seasons (except for the winter months), mainly during spring and summer, concurrently with mature females. This synchrony suggested that populations could be sexually segregated and mating could occur prior to egg-laying. It is known that the Rajidae family members (e.g., *R. miraletus* and *D. oxyrinchus*, Marongiu et al., 2015) do not preserve sperm for a long time in the oviducal glands as result of a recent mating episode, which could explain the presence of capable of reproducing females concurrently with active males.

The reproductive seasonality among oviparous chondrichthyans is less common than among viviparous ones. Two general reproductive strategies have been observed in oviparous species: reproduction throughout the year with one or two egg-laying peaks and a well-defined egg-laying season (Hamlett and Koob, 1999; Wyffels, 2009). The general rule among skates is to lay eggs throughout the year (Frisk, 2010). In particular, this strategy is known for four species inhabiting the Mediterranean Sea: *D. nidarosiensis* (Follesa et al., 2012), *D. oxyrinchus* (Bellodi et al., 2017), *R. clavata* (Capapé et al., 2007; Kadri et al., 2014), and *R. miraletus* (Ungaro, 2004; Kadri et al., 2012). Seasonal egg laying, here reported, appears uncommon and it has only been currently observed in two other skates, *R. asterias* (Barone et al., 2007) and *R. brachyura* (Porcu et al., 2015). These species have a shallow, coastal habit (<100 m depth) subject to seasonal variability in common, different from the Speckled skate which shows a wider depth range (18–660 m in Sardinian seas). However, the reproductive seasonality of *R. polystigma* could be linked to the clear preference of extruding females, for continental shelf sandy bottoms as egg-laying sites, which are deeply influenced by environmental factors, as recorded by Porcu et al. (2017).

The estimated ovarian fecundity (14–19 ripe follicles) appeared lower than that observed on Tunisian coasts by Capapé and Quignard (1978) (20–62). This high discrepancy could be due to a different methodology used by the authors who may have considered all follicles (immature and mature) in the fecundity estimation.

4.4. Segregation patterns

Depth was the main factor that influenced segregation patterns in *R. polystigma.* Even if no evidence of segregation by sex was observed, a distribution pattern during different life stages has been recorded. *R. polystigma* appears to complete its life cycle in impacted coastal waters, with adults found exclusively in shallows while immature specimens were found in the whole bathymetric range of the species. The presence of the almost total concentration of active males and mature females in the upper bathymetric layer (<100 m) suggests that mating occurs in shallow waters where extruding females were also found. For mature and extruding females, remaining in shallow waters could be advantageous because high temperatures are thought to provide thermal physiological benefits such as increased embryonic growth rates (Economakis and Lobel, 1998; Hight and Lowe, 2007). This pattern may justify the egg-laying during warm months observed in this study. Considering species with a wide bathymetric range such as *R. polystigma* (18–660 m, present study), this behaviour seems to be opposite to that observed among chondrichtyans inhabiting the Mediterranean Sea, where mature females were mostly found in deep waters (e.g., Follesa et al., 2012; Porcu et al., 2014; Cau et al., 2016; Bellodi et al., 2017).

5. Conclusion

The growth patterns found in this study indicate that *R. polystigma* is a relatively short-lived and fast-growing species if compared with other Rajids (e.g. Porcu et al., 2015; Bellodi et al., 2017). These features could ascribe this skate as more resilient to exploitation than other elasmobranchs for any given level of fishing pressure. Similarly, reproductive aspects of *Raja polystigma* (e.g., late size and age at maturity, low fecundity and high dependence on the coastal environment, seasonal reproductive period when the maximum exploitation is observed) highlights the high vulnerability of this species (Dulvy and Reynolds, 2002). For this reason, measures to alleviate anthropic effects on this habitat are urgently needed. The identification of important areas in the life cycle of *R. polystigma*, the regulation of the fishing effort, and promotion of live release of this by-catch, vulnerable species should be included.

Declaration of competing interest

The authors declare that they have no known competing financial interests or personal relationships that could have appeared to influence the work reported in this paper.

CRediT authorship contribution statement

Cristina Porcu: Conceptualization, Methodology, Writing - original draft, Writing - review & editing, Software, Investigation. **Andrea Bellodi:** Conceptualization, Methodology, Writing - original draft, Software, Investigation. **Alessandro Cau:** Formal analysis, Investigation. **Rita Cannas:** Formal analysis, Investigation. **Martina F. Marongiu:** Formal analysis, Investigation, Writing - review & editing. **Antonello Mulas:** Formal analysis, investigation. **Maria C. Follesa:** Conceptualization, Methodology, Writing - original draft, Funding acquisition, Project administration, Supervision.

Acknowledgements

This study was financed by Autonomous Region of Sardinia within the frame of the research project 'Approccio multidisciplinare per la conservazione e gestione della selacofauna del Mediterraneo' (LR7 CRP- 25321) and carried out within the Data Collection Regulation and Framework - module trawl surveys MEDITS (Mediterranean International Trawl Survey).

References

Akaike, H., 1974. A new look at the statistical model identification. IEEE Trans. Automat. Control 19, 716–723. http://dx.doi.org/10.1109/TAC.1974.1100705.

Araya, M., Cubillos, L.A., 2006. Evidence of two-phase growth in elasmobranchs. Environ. Biol. Fish. 77, 293–300.

A.V.V.A., 2016. MEDITS-Handbook. Version N. 8. MEDITS Working Group, p. 177.

Barnett, L.A.K., Winton, M.V., Ainsley, S.M., Cailliet, G.M., Ebert, D.A., 2013. Comparative demography of skates: Life-history correlates of productivity and implications for management. PLoS ONE 8 (5), e65000. http://dx.doi.org/10.1371/journal.pone.0065000.

Barone, M., De Ranieri, S., Fabiani, O., Pirone, A., Serena, F., 2007. Gametogenesis and maturity scale of *Raja asterias* Delaroche, 1809 (Chondrichthyes, Rajidae) from the South Ligurian Sea. Hydrobiol. 580, 245–254.

Beamish, R.J., Fournier, D.A., 1981. A method for comparing the precision of a set of age determinations. Can. J. Fish. Aquat. Sci. 38, 982–983. http://dx.doi.org/10.1139/f81-132.

Bellodi, A., Porcu, C., Cannas, R., Cau, Al., Marongiu, M.F., Mulas, A., Vittori, S., Follesa, M.C., 2017. Life–history traits of the long–nosed skate *Dipturus oxyrinchus*. J. Fish Biol. 90, 867–888.

von Bertalanffy, L., 1938. A quantitative theory of organic growth (inquires of growth laws II). Hum. Biol. 10, 181–183.

Caillet, G.M., Martin, L.K., Kusher, D., Wolf, P., Welden, B., 1983. Techniques for Enhancing Vertebral Bands in Age Estimation of California Elasmobranchs, Vol. 8. US Dept. of Coerce NOAA Technical report, NMFS, pp. 157–165.

Cailliet, G.M., Goldman, K., 2004. Age determination and validation in chondrichthyan fishes. In: Carrier, J.C., Musick, J.A., Heithaus, M.R. (Eds.), Biology of Sharks and their Relatives. CRC Press LLC, Boca Raton, pp. 399–447.

Campana, S.E., 2014. Age determination of elasmobranchs, with special reference to Mediterranean species: a technical manual. In: Studies and Reviews. General Fisheries Commission for the Mediterranean. No. 94. FAO, Rome, p. 38.

Cannas, R., Pasolini, P., Mancusi, C., Follesa, M.C., et al., 2008. Distribution, molecular systematics and phylogeography of *Raja polystigma* and *Raja montagui* in the Mediterranean. Biol. Mar. Mediterr. 15, 188–191.

Capapé, C., Guelorget, O., Siau, Y., Vergne, Y., Quignard, J.P., 2007. Reproductive biology of the thornback ray *Raja clavata* (Chondrichtyes: Rajidae) from the coast of Languedoc (Southern France, Northern Mediterranean). Vie Milieu 57, 83–90.

Capapé, C., Quignard, J.P., 1978. Contribution a la biologie des rajidae des côtes tunisiennes. XIV - *Raja polystigma* Regan, 1923. Répartition géographique et bathymétrique, sexualité, reproduction, fécondité. Cah. Biol. Mar. 19, 233–244.

Carbonara, P., Follesa, M.C. (Eds.), 2019. Handbook on Fish Age Determination: A Mediterranean Experience. Studies and Reviews. n. 98. FAO, Rome, p. 180.

Cau, A., Follesa, M.C., Moccia, D., Bellodi, A., Mulas, A., Bo, M., Canese, S., Angiolillo, M., Cannas, R., 2016. *Leiopathes glaberrima* millennial forest from SW Sardinia as nursery ground for the small spotted catshark *Scyliorhinus canicula*. Aquat. Conserv.: Mar. Freshw. Ecosyst. 27, 731–735.

Chang, W.Y.B., 1982. A statistical method for evaluating the reproducibility of age determination. Can. J. Fish. Aquat. Sci. 39, 1208–1210.

Clarke, K.R., Gorley, R.N., 2006. PRIMER V6: User Manual/Tutorial (Plymouth Routines in Multivariate Ecological Research). PRIMER-E, Plymouth.

Coll, M., Piroddi, C., Steenbeek, J., Kaschner, K., et al., 2010. The biodiversity of the Mediterranean Sea: estimates, patterns, and threats. PLoS ONE 5, http://dx.doi.org/10.1371/journal.pone.0011842, e11842.

Cortés, E., 2002. Stock Assessment of Small Coastal Sharks in the US Atlantic and Gulf of Mexico. NOAA, National Marine Fisheries Service, Panama City.

Dulvy, N.K., Allen, D.J., Ralph, G.M., Walls, R.H.L., 2016. The Conservation Status of Sharks, Rays and Chimaeras in the Mediterranean Sea [Brochure]. IUCN, Malaga, Spain.

Dulvy, N.K., Reynolds, J.D., 2002. Predicting extinction vulnerability in skates. Conserv. Biol. 16, 440–450. http://dx.doi.org/10.1046/j.1523-1739.2002.00416.x.

Dulvy, N.K., Sadovy, Y., Reynolds, J.D., 2003. Extinction vulnerability in marine populations. Fish Fish. 4, 25–64. http://dx.doi.org/10.1046/j.1467-2979.2003.00105.x.

Ebert, D.A., Compagno, L.J.V., Cowley, P.D., 2008. Aspects of the reproductive biology of skates (Chondrichthyes: Rajiformes: Rajoidei) from southern Africa. ICES J. Mar. Sci. 65, 81–102.

Ebert, D.A., Maurer, J.R., Ainsley, S.M., Barnett, L.A.K., Cailliet, G.M., 2009. Life history and population dynamics of four endemic alaskan skates: determining essential biological information for effective management of bycatch and target species. In: North Pacific Research Board Final Report. p. 715.

Economakis, A.E., Lobel, P.S., 1998. Aggregation behavior of the grey reef shark, Carcharhinus amblyrhynchos, at Johnston Atoll, Central Pacific Ocean. Environ. Biol. Fish. 51, 129–139.

Ellis, J.R., Silva, J.F., McCully, S.R., Evans, M., Catchpole, T., 2010. UK Fisheries for Skates (Rajidae): History and Development of the Fishery, Recent Management Actions and Survivorship of Discards. ICES Document CM 2010/E: 10, p. 38.

Eltink, A.T.G.W., 2000. Age reading comparisons (MS Excel workbook version 1.0 October 2000). Available at http://www.efan.no/.

Fabens, A.J., 1965. Properties and fitting of the von Bertalanffy growth curve. Growth 29, 265–289.

Ferretti, F., Myers, R.A., 2006. By-Catch of sharks in the Mediterranean Sea: available mitigation tools. In: Proceedings of the Workshop on the Mediterranean Cartilaginous Fish with Emphasis on Southern and Eastern Mediterranean, Istanbul, Turkey, pp. 158–169.

Fisher, R.A., Call, G.C., Grubbs, R.D., 2013. Age, growth and reproductive biology of cownose rays in Chesapeake Bay. Mar. Coast. Fish. 5, 224–235. http://dx.doi.org/10.1080/19425120.2013.812587.

Follesa, M.C., Agus, B., Bellodi, A., Cannas, R., Capezzuto, F., Casciaro, L., Cau, A., Cuccu, D., Donnaloia, M., Fernandez-Arcaya, U., Gancitano, V., Gaudio, P., Marongiu, M.F., Mulas, A., Pesci, P., Porcu, C., Rossetti, I., Sion, L., Vallisneri, M., Carbonara, P., 2019a. The MEDITS maturity scales as a useful tool for investigating the reproductive traits of key species in the Mediterranean Sea. Sci. Mar. 83S1, 235–256.

Follesa, M.C., Cannas, R., Cabiddu, S., Cau, Al., Mulas, A., Porcu, C., Cau, A., 2012. Preliminary observations of the reproductive biology and diet for the Norwegian skate *Dipturus nidarosiensis* (Rajidae) from the Central Western Mediterranean Sea. Cybium 36 (3), 473–477.

Follesa, M.C., Marongiu, M.F., Zupa, W., Bellodi, A., Cau, A., Cannas, R., Colloca, F., Djurovic, M., Isajlovic, I., Jadaud, A., Manfredi, C., Mulas, A., Peristeraki, P., Porcu, C., Ramirez-Amaro, S., Salmerón Jiménez, F., Serena, F., Sion, L., Thasitis, I., Cau, A., Carbonara, P., 2019b. Spatial variability of Chondrichthyes in the northern Mediterranean. Sci. Mar. 83S1, 81–100.

Follesa, M.C. and Carbonara, P., (Eds.), 2019. *Atlas of the maturity stages of Mediterranean fishery resources*, Studies and Reviews N. 99. Rome, FAO. 268.

Frisk, M.G., 2010. Life history strategies of batoids. In: Carrier, J.C., Musick, M.R. (Eds.), Sharks and their Relatives II: Biodiversity, Adaptive Physiology, and Conservation. CRC Press, Boca Raton, pp. 283–316.

Frisk, M.G., Miller, T.J., 2009. Maturation of little skate and winter skate in the western atlantic from cape hatteras to georges bank. Mar. Coast. Fish. 1, 1–10.

Frodella, N., Cannas, R., Velonà, A., Carbonara, P., et al., 2016. Population connectivity and phylogeography of the Mediterranean endemic skate *Raja polystigma* and evidence of its hybridization with the parapatric sibling *R. montagui*. Mar. Ecol. Prog. Ser. 554, 99–113. http://dx.doi.org/10.3354/meps11799.

Goldman, K.J., 2005. Age and growth of Elasmobranch fishes. In: Musick, J.A., Bonfil, R. (Eds.), Management Techniques for Elasmobranch Fisheries. FAO Fisheries Technical Paper 474, FAO, Rome, pp. 76–102, Available at http://www.fao.org/docrep/009/a0212e/a0212e00.htm/.

Goosen, A.J.J., Smale, M.J., 1997. A preliminary study of age and growth of the smoothhound shark *Mustelus mustelus* (Triakidae). South Afr. J. Mar. Sci. 18, 5–92.

Haddor, M., 2001. Modelling and Quantitative Methods in Fisheries. CRC Press, Boca Raton, FL.

Hamlett, W.C., Koob, T.J., 1999. Female reproductive system. In: Hamlett, W.C. (Ed.), Sharks, Skates, and Rays: The Biology of Elasmobranch Fishes. Johns Hopkins University Press, Baltimore, pp. 398–443.

Henderson, P.A., Seaby, R.M., 2006. Growth II. Pisces Conservation Ltd, Lymington, Available at http://www.pisces-conservation.com/.

Hight, B.V., Lowe, C.G., 2007. Elevated body temperatures of adult female leopardsharks, *Triakis semifasciata*, while aggregating in shallow nearshore embay-ments: evidence for behavioral thermoregulation?. J. Exp. Mar. Biol. Ecol. 352, 114–128.

Holden, M.J., 1974. Problems in the rational exploitation of elasmobranch populations and some suggested solutions. In: Jones, E.H. (Ed.), Sea Fisheries Research. Wiley and Sons, New York, pp. 187–215.

ICES, 2008. Report of the Workshop on Maturity Ogive Estimation for Stock Assessment (WKMOG), 3–6 June 2008, Lisbon, Portugal. p. 72.

Kadri, H., Marouani, S., Saïdi, B., Bradai, M.N., Bouaïn, A., Morize, E., 2014. Age, growth, sexual maturity and reproduction of the thornback ray, *Raja clavata* (L.), of the Gulf of Gabès (south–central Mediterranean Sea). Mar. Biol. Res. 10 (4), 416–425.

Kadri, H., Marouani, S., Saidi, B., Bradai, M.N., Ghorbel, M., Bouain, A., Eric, M., 2012. Age, growth and reproduction of *Raja miraletus* (Linnaeus, 1758) (Chondrichthyes: Rajidae) of the Gulf of Gabès (Tunisia, Central Mediterranean Sea). Mar. Biol. Res. 8, 309–317.

LaMarca, M.J., 1966. A simple technique for demonstrating calcified annuli in the vertebrae of large elasmobranchs. Copeia 351–352.

Mabragaña, E., Lucifora, L.O., Corbo, M.L., Díaz de Astarloa, J.M., 2015. Seasonal reproductive biology of the bignose fanskate *Sympterygia acuta* (Chondrichthyes, Rajidae). Estuar. Coast. 38, 1466–1476. http://dx.doi.org/10.1007/s12237-014-9888-0.

Marongiu, M.F., Porcu, C., Bellodi, A., Cannas, R., Cau, A., Cuccu, D., Mulas, A., Follesa, M.C., 2017. Temporal dynamics of demersal chondrichthyan species in the central western Mediterranean Sea: The case study in Sardinia Island. Fish. Res. 193, 81–94. http://dx.doi.org/10.1016/j.fishres.2017.04.001.

Marongiu, M.F., Porcu, C., Bellodi, A., Cuccu, D., Mulas, A., Follesa, M.C., 2015. Oviducal gland microstructure of two Rajidae species, *Raja miraletus* and *Dipturus oxyrinchus*. J. Morph. 76, 1392–1403.

McKinney, M.L., 1999. High rates of extinction and threat in poorly studied taxa. Conserv. Biol. 13, 1273–1281. http://dx.doi.org/10.1046/j.1523-1739.1999.97393.x.

McPhie, R.P., Campana, S.E., 2009. Reproductive characteristics and population decline of four species of skate (Rajidae) off the eastern coast of Canada. J. Fish Biol. 75, 223–246.

Mejía-Falla, P.A., Cortés, E., Navia1, A.F., Zapata, F.A., 2014. Age and growth of the round stingray *Urotrygon rogersi*, a particularly fast-growing and short-lived elasmobranch. PLoS One 9 (4), e96077. http://dx.doi.org/10.1371/journal.pone.0096077.

Mulas, A., Bellodi, A., Cannas, R., Carbonara, C., Cau, A., Marongiu, M.F., Pesci, P., Porcu, C., Follesa, M.C., 2019. Resource partitioning among sympatric elasmobranchs in the central-western Mediterranean continental shelf. Mar. Biol. 166, 153. http://dx.doi.org/10.1007/s00227-019-3607-0.

Mulas, A., Bellodi, A., Cannas, R., Cau, A., Cuccu, D., Marongiu, M.F., Porcu, C., Follesa, M.C., 2015. Diet and feeding behaviour of long-nosed skate *Dipturus oxyrinchus* in sardinian waters (central-western Mediterranean). J. Fish Biol. 86, 121–138. http://dx.doi.org/10.1111/jfb.12551.

Neer, J.A., Thompson, B.A., 2005. Life history of the Cownose ray, *Rhinoptera bonasus*, in the northern Gulf of Mexico, with comments on geographic variability in life history traits. Environ. Biol. Fish. 73, 321–331. http://dx.doi.org/10.1007/s10641-005-2136-5.

Oddone, M.C., Vooren, C.M., 2005. Reproductive biology of *Atlantoraja cyclophora* (Regan 1903) (Elasmobranchii: Rajidae) off southern Brazil. ICES J. Mar. Sci. 62, 1095–1103.

Porcu, C., Bellodi, A., Cannas, R., Marongiu, M.F., Mulas, A., Follesa, M.C., 2015. Life–history traits of the commercial blonde ray, *Raja brachyura*, from the central–western Mediterranean Sea. Mediterr. Mar. Sci. 16 (1), 90–102.

Porcu, C., Marongiu, M.F., Bellodi, A., Cannas, R., Cau, A., Melis, R., Mulas, A., Soldovilla, G., Vacca, L., Follesa, M.C., 2017. Morphological descriptions of the eggcases of skates (Rajidae) from the central–western Mediterranean, with notes on their distribution. Helgol. Mar. Res. 71, 10.

Porcu, C., Marongiu, M.F., Follesa, M.C., Bellodi, A., Mulas, A., Pesci, P., Cau, A., 2014. Reproductive aspects of the velvet belly *Etmopterus spinax* (Chondrichthyes: Etmopteridae), from the central western Mediterranean Sea. Notes on gametogenesis and oviducal gland microstructure. Mediterr. Mar. Sci. 15 (2), 313–326.

R Core Team. R: A, 2017. Language and environment for statistical computing.

Ramírez-Amaro, S., Ordines, F., Picornell, A., Castro, J.A., Ramon, C., Massutí, E., Terrasa, B., 2018. The evolutionary history of Mediterranean Batoidea (Chondrichthyes: Neoselachii). Zool. Scr. 1–13. http://dx.doi.org/10.1111/zsc.12315.

Richards, F.J., 1959. A flexible growth function for empirical use. J. Exp. Bot. 10, 290–301. http://dx.doi.org/10.1093/jxb/10.2.290.

Ricker, W.E., 1979. Growth rates and models. In: Hoar, W.S., Randall, D.J., Brett, J.R. (Eds.), Fish Physiology: Bioenergetics and Growth. Academic Press, New York, pp. 677–743.

Roberts, C.M., Hawkins, J.P., 1999. Extinction risk in the sea. Trends Ecol. Evol. 14, 241–246. http://dx.doi.org/10.1016/S0169-5347(98)01584-5.

Rohlf, F.J., 2005. TpsDig, digitize landmarks and outlines, version 2.16. In: Department of Ecology and Evolution. State University of New York at Stony Brook.

Serena, F., 2005. Field identification guide to the sharks and rays of the Mediterranean and Black Sea. In: FAO Species Identification Guide for Fishery Purposes. FAO, Rome.

Serena, F., Mancusi, C., Barone, M., 2010. Field identification guide to the skates (Rajidae) of the Mediterranean Sea: guidelines for data collection and analysis. Biol. Mar. Mediterr. 17 (2), 204.

Stevens, J.D., 1975. Vertebral rings as a means of age determination in the blue shark (*Prionace glauca* L.). J. Mar. Biol. Assoc. U.K. 55, 657–665.

Sulikowski, J.A., Irvine, S.B., DeValerio, K.C., Carlson, J.K., 2007. Age, growth and maturity of the roundel skate, *Raja texana*, from the Gulf of Mexico, USA. Mar. Freshw. Res. 58 (1), 41–53.

Sulikowski, J.A., Morin, M.D., Suk, S.H., Howell, W., 2003. Age and growth estimates of the winter skate (*Leucoraja ocellata*) in the western Gulf of Maine. Fish. Bull. 101, 405–413.

Thorson, J.T., Simpfendorfer, C.A., 2009. Gear selectivity and sample size effects on growth curve selection in shark age and growth studies. Fish. Res. 98, 75–84.

Ungaro, N., 2004. Biological parameters of the brown ray, *Raja miraletus*, in the Southern Adriatic basin. Cybium 28 (2), 174–176.

Valls, M., Quetglas, A., Ordines, F., Moranta, J., 2011. Feeding ecology of demersal elasmobranchs from the shelf and slope off the Balearic Sea (Western Mediterranean). Sci. Mar. 75 (4), 633–639. http://dx.doi.org/10.3989/scimar.2011.75n463.

Winsor, C., 1932. The Gompertz curve as a growth equation. Proc. Natl. Acad. Sci. USA 18, 1–8.

Wyffels, J.T., 2009. Embryonic development of Chondrichthyan fishes—a review. In: Kunz, Y.W., Luer, C.A., Kapoor, B.G. (Eds.), Development in Non-Teleost Fishes. Enfield: Science Publishers, pp. 1–103.

Yigin, C., Ismen, A., 2010. Age, growth, reproduction and feed of long-nosed skate, *Dipturus oxyrinchus* (Linnaeus 1758) in Saros Bay, the north Aegean Sea. J. Appl. Ichthyol. 26, 913–919. http://dx.doi.org/10.1111/j.1439-0426.2010.01510.x.

Zar, J.H., 1999. Biostatistical Analysis, fourth ed. Prentice Hall, Upper Saddle River, NJ, p. 663.

Zeiner, S.J., Wolf, P., 1993. Growth characteristics and estimates of age at maturity of two species of skates (*Raja binoculata* and *Raja rhina*) from Monterey Bay, California. In: Branstetter, S. (Ed.), Conservation Biology of Elasmobranchs. (Ed.). NOAA Technical Reports NMFS 115, pp. 87–99, Available at http://spo.nmfs.noaa.gov/tr115.pdf/.